Plasma Angular Momentum Loss by MHD Mode Locking

Hartmut Zohm, Arne Kallenbach, Hardo Bruhns,
Gerd Fußmann, Otto Klüber

IPP 1/251 December 1989

MAX-PLANCK-INSTITUT FÜR PLASMAPHYSIK

8046 GARCHING BEI MÜNCHEN

MAX-PLANCK-INSTITUT FÜR PLASMAPHYSIK

GARCHING BEI MÜNCHEN

Plasma Angular Momentum Loss by MHD Mode Locking

Hartmut Zohm, Arne Kallenbach, Hardo Bruhns,
Gerd Fußmann, Otto Klüber

IPP 1/251 December 1989

Die nachstehende Arbeit wurde im Rahmen des Vertrages zwischen dem Max-Planck-Institut für Plasmaphysik und der Europäischen Atomgemeinschaft über die Zusammenarbeit auf dem Gebiete der Plasmaphysik durchgeführt.

Plasma Angular Momentum Loss by MHD Mode Locking

H. Zohm, A. Kallenbach, H. Bruhns, G. Fussmann, O. Klüber
Max-Planck-Institut für Plasmaphysik, EURATOM Association,
D-8046 Garching, Fed. Rep. of Germany

PACS 52.30 Plasma flow, MHD
PACS 52.35 Plasma instabilities
PACS 52.55G Plasma in torus

Abstract: The loss of angular momentum of a rotating plasma due to mode locking is investigated using spectroscopic rotation measurements and magnetic probe data. The electromagnetic force on the plasma regarding both the interaction with the resistive vessel wall and the error field is calculated. Simulations of the temporal evolution of the toroidal bulk rotation by solving the momentum transport equation in the presence of the magnetic forces explain the toroidal momentum balance in detail. As a result we find that the plasma within the island is affected by the electromagnetic force, while the rest of the plasma is slowed down by viscous coupling.

In Tokamaks the m=2, n=1 tearing mode plays an important role as a precursor to disruptions. In various experiments, this mode, which is normally rotating, is observed to come to rest if the magnetic field perturbation reaches a sufficient strength (mode locking) /1/. This is of importance for the analysis of the momentum transport in plasmas, which cannot be applied in the usual way in the case of MHD mode locking /2/. On the other hand theory predicts a further destabilization of tearing modes in the case of mode locking due to the absence of wall-stabilizing effects /3/, which eventually may lead to a disruption.

The mode frequency is due to the sum of the reduced electron diamagnetic drift and the macroscopic velocity /4/. As the perturbation has constant phase along the field lines, only the propagation normal to the magnetic field lines can be observed:

$$\vec{u} = \vec{v}_\perp + \frac{\vec{\nabla} p_i \times \vec{B}}{n_e e B^2} \tag{1}$$

where $\vec{u}$ denotes the phase velocity of the mode and $\vec{v}_\perp$ is the plasma bulk velocity normal to the magnetic field $\vec{B}$.

There are two forces acting on rotating MHD-modes: One is due to the interaction with the resistive wall of the vacuum vessel /5/. It results the $\vec{j} \times \vec{B}$ force of the currents induced in the vessel wall with the radial field of the perturbation, which can be written as

$$F_{rw} = -4\pi^2 \frac{B_r^2 r_{res}^2 R_0}{\mu_0 b} \left(\frac{r_{res}}{b}\right)^{2m-1} \frac{\Omega\tau}{1+(\Omega\tau)^2} \tag{2}$$

where B_r is the radial component of the perturbed field on the resonant surface located at r_{res}, τ the resistive skin time of the vessel of aspect ratio $\frac{R_0}{b}$ and $\Omega = \dot{\theta}$ the angular frequency of the rotating mode. The force has a maximum for $\Omega\tau = 1$. This corresponds to a signal frequency of about 50 Hz in the ASDEX case which is well below the observed MHD mode frequencies of at least 1 kHz.

The second force on the mode is due to errors in the positioning and the shape of the field coils producing the vacuum field configuration. A (m,n) mode mainly interacts with the (m,n) component of the error field. If this error field is assumed to be produced by an external helical current I_{ext} located at the plasma boundary $r = a$, the force can be written as /6/

$$F_{ef} = -\pi^2 R_0 m \frac{a}{r_{res}} I_{ext} B_r(a) \sin\left(m\theta(t)\right). \tag{3}$$

Here $B_r(a)$ denotes the field perturbation at the plasma boundary; θ is the angle between the static modulation produced by the error field and the rotating mode island.

To study the effect of these forces on the plasma motion, in a first step we numerically integrate the equation of motion for the mode

$$T\frac{d^2\theta}{dt^2} = (F_{rw} + F_{ef})R_0, \tag{4}$$

where T is the moment of inertia of the island structure. Here, an initial mode rotation is assumed and neither driving terms nor viscous effects are included. We use experimental data for the temporal evolution of B_r and T to simulate the behaviour of the angular velocity Ω (see Fig. 1). The force given by eq.(3) introduces a periodic modulation of the angular frequency. The amplitude of the modulation is proportional to $\sqrt{I_{ext}}$. If for given values of B_r and I_{ext} this amplitude becomes comparable to the mean rotation frequency, the actual angular velocity can get close to the inverse of the resistive skin time τ of the vessel while the mean rotation frequency detected by the Mirnov coils is still much higher than τ^{-1}. In this case, the resistive wall force becomes large and mode locking

occurs. Therefore the mean rotation frequency always exhibits a lower limit, which is equal to the amplitude of the frequency modulation at the time where mode locking occurs. Thus the value of I_{ext} can be inferred from the lower limit of rotation frequency before mode locking.

In the ASDEX device, mode locking is frequently observed, especially during lower hybrid current drive (LHCD). The shape of the Mirnov signals before mode locking shows strong deviations from sinusoidal due to the modulation of the angular velocity mentioned above. Simulating the interaction with the error field using eq.(3) reproduces the observed signals in detail (see. Fig. 2). For this particular shot, the lower limit of rotation frequency is about 750 Hz leading to a value of $I_{ext} = 310A$ for the amplitude of the (2,1) component of the external error field. Comparing the shape of the Mirnov signals with the simulation (Fig. 2), we can also determine the position of the island created by the error field with respect to the vessel and hence explain the position of the locked mode relative to the vessel: Analysis of magnetic probe data on ASDEX shows that this position corresponds to a phase of $m\theta = 0.96\pi$ in eq.(3). In this sense mode locking means that the angular momentum of the mode is marginally insufficient to reach the region where the force given by eq.(3) is positive, i.e. accelerating the plasma with respect to the vessel frame. As the error field structure determined by mechanical inaccurracies is static, mode locking should occur always in the same position. This agrees with the observation in ASDEX.

For a detailed explanation of the experiment, problems arise concerning the question whether the form of the equation of motion for the rotating mode eq.(4) is appropriate. The forces on the mode are exerted perpendicular to $\vec{B}$, i.e. mainly poloidal. On the other hand, poloidal rotation should undergo strong neoclassical damping /7/. We therefore restrict ourselves to a purely toroidal force balance for the macroscopic rotation. In the following we consider only cases where the toroidal velocity is dominating due to strong neutral beam injection (NBI) which we now regard as an additional term (driving force) in eq.(4).

To solve eq.(4) we use a code for the radial diffusion of the angular momentum supplied to the plasma by NBI in the presence of the magnetic forces described by eq.(2) and eq.(3). A simplified model is applied for the momentum deposition by the neutral beams, namely that the location of momentum deposition is equal to the radial position where ionization occurs. We use measured ASDEX data for the perturbed magnetic field from Mirnov coils under the assumption that the field of the plasma perturbation decays like a vacuum field outside the q=2 surface and apply toroidal rotation profiles measured by charge exchange recombination spectroscopy (CXRS) with a temporal resolution of 50 ms /2/ as well as density

profiles obtained by a YAG Thomson scattering system /8/. Within the magnetic islands, the plasma is directly slowed down by the electromagnetic forces. Outside the islands, the plasma rotation is affected by viscous coupling between neighbouring flux surfaces. The viscosity is determined from a transport analysis of the rotation data at a time where no mode is present. Eq. (1) shows that mode locking ($\vec{u} = 0$) also means a flattening of the ion pressure over the island region leading to a new three dimensional plasma configuration. This can be explained by the enhanced transport within the island region. Experimental studies dedicated to this subject are in progress; the results being not yet available, we assume in the simulations that the diffusion coefficient in the island region is enhanced by a factor of 10. Fig. 3 a) shows the temporal evolution of an NBI-heated ASDEX shot where mode locking occurs. The results of a simulation of the toroidal rotation for the same discharge is shown in Fig. 3 c). As can be seen, the q=2 region (r=37 cm) is calculated to lock on the same time scale as in the experiment. The measured behaviour of the plasma bulk rotation (Fig. 3 b)) cannot be explained by viscous effects alone, since the rotation velocity of the central region is only slightly affected when the motion of the q=2 island near the boundary goes to zero. From SX-measurements, however, a large m=1 mode in the plasma center is detected, which is coupled to the (2,1) mode such that this mode imposes its frequency onto the (1,1) mode. In the model, mode coupling is simulated by splitting up the force originally exerted only on the (2,1) island onto both modes. To reproduce the evolution of the rotation profile we have to assume that one third of the force acts on the m=1 island. The field perturbation of the m=1 internal kink is not seen on the Mirnov probes; hence, a direct interaction of this mode with the vessel wall, if any, is small. Using this model, the rotation profile obtained from the simulation reproduces the experimental data (Fig. 3 b)) reasonably well.

Varying the value of I_{ext} in the simulations within the range of the experimental error bars (30%) leads to significant differences between the simulations and the experiments. If for example in the simulation I_{ext} is reduced by 30%, mode locking cannot be reproduced. This may explain why mode locking is not a general feature of ASDEX shots but rather is observed as a limit on the operational regime.

Fig. 4 shows another example of a comparison between the simulation of the toroidal force balance and the experiment. The selected shot develops a locked mode during LHCD; unlocking is produced by NBI. From the available experimental data, the temporal evolution of this shot can also be investigated. On the measured rotation profile it can be seen that the q=2 surface is retarded by the electromagnetic forces while the rest of the plasma is accelerated by the beams. In

this case no significant m=1 mode is observed experimentally so that the central rotation should be only damped by the viscous effect which is consistent with the experimentally observed rotation profile.

In summary we conclude that the toroidal force balance for MHD mode locking is well described by our model, which includes both the electromagnetic forces due to interaction with a resistive wall and error fields as well as the viscous coupling between the island structure and the bulk plasma. Further investigations have to be performed to analyse the mode coupling which here has been included only empirically.

We gratefully acknowledge the help of M. Kornherr in analysing the SX-Data as well as the work of the whole ASDEX-Team. Special thanks are due to K. Lackner for a helpful discussion.

References:

/1/ Snipes, J.A. et al, Nucl. Fus., Vol.28, 1085 (1988); Hutchinson, I. H., Overskei, D. O., IAEA Symp. on Current Disruptions in toroidal devices, Garching, IPP Report 3/51 (1979)

/2/ Kallenbach, A. et al.: Improvement of Angular Momentum Confinement with Density Peaking on ASDEX, accepted for publication in Nucl. Fus.

/3/ Persson, M.; Bondeson, A., Nucl. Fus., Vol.29, 989 (1989)

/4/ Klüber, O.; Zohm, H.; Bruhns, H.; Gernhardt, J.; Kallenbach, A.; Zehrfeld, H.P.: MHD Mode Structure and Propagation in the ASDEX Device, IPP Report III/140 (1989), to be submitted to Nucl. Fus.

/5/ Nave, M.F.F.; Wesson J., Controlled Fusion and Plasma Physics (Proc. 14th Eur. Conf. Madrid, 1103 (1987))

/6/ Hender, T.C.; Gimblett, C.G.; Robinson, D.C., Controlled Fusion and Plasma Physics (Proc. 15th Eur. Conf. Dubrovnik, 437 (1988))

/7/ Stix, T.H., Phys. of Fluids, Vol.16, 1260 (1973)

/8/ Röhr, H.; Steuer, K.-H.; Murmann, H.; Meisel, D.: Periodische Vielkanal-Thomson-Streuung, IPP Report III/121 (1987)

Figure Captions

Fig. 1: Simulated temporal behaviour of the angular velocity and the mean rotation frequency during mode locking taking into account the resistive wall and the error field. Note that the mean rotation frequency drops abruptly from its lower limit value to zero.

Fig. 2: Measured (a) and simulated (b) Mirnov signals from coils at different poloidal angles for an ASDEX shot showing mode locking. To demonstrate the

modulation of the signals, in the simulation only the error field force was included, therefore it was not tried to reproduce mode locking as seen in Fig. 2 a).

Fig. 3: Measured Mirnov signals, NBI power, plasma current (a) and rotation profiles (b) before and after mode locking compared to the simulated profile after mode locking (t=1.75s) and evolution of rotation at different radii (c). The MHD mode leading to mode locking is seen on the Mirnov trace at t=1.73 s. The shot terminated due to a disruption at t=1.78 s. The spikes on the Mirnov signal at t=1.78 s and t=1.82 s are due to the inward motion of the plasma during the disruption.

Fig. 4: Unlocking of a locked mode by NBI: Mirnov trace and additional heating power (a), rotation profiles measured directly after unlocking compared to the simulated profile at t=1.55 s (b) and temporal evolution of the rotation at different radii (c). In (b) a rotation profile for a reference shot without a locked mode is shown. In the simulation, at t=1.5 s the plasma was assumed to be resting, mode locking is seen on the Mirnov trace from t=1.508 s to t=1.522 s.

Fig. 1

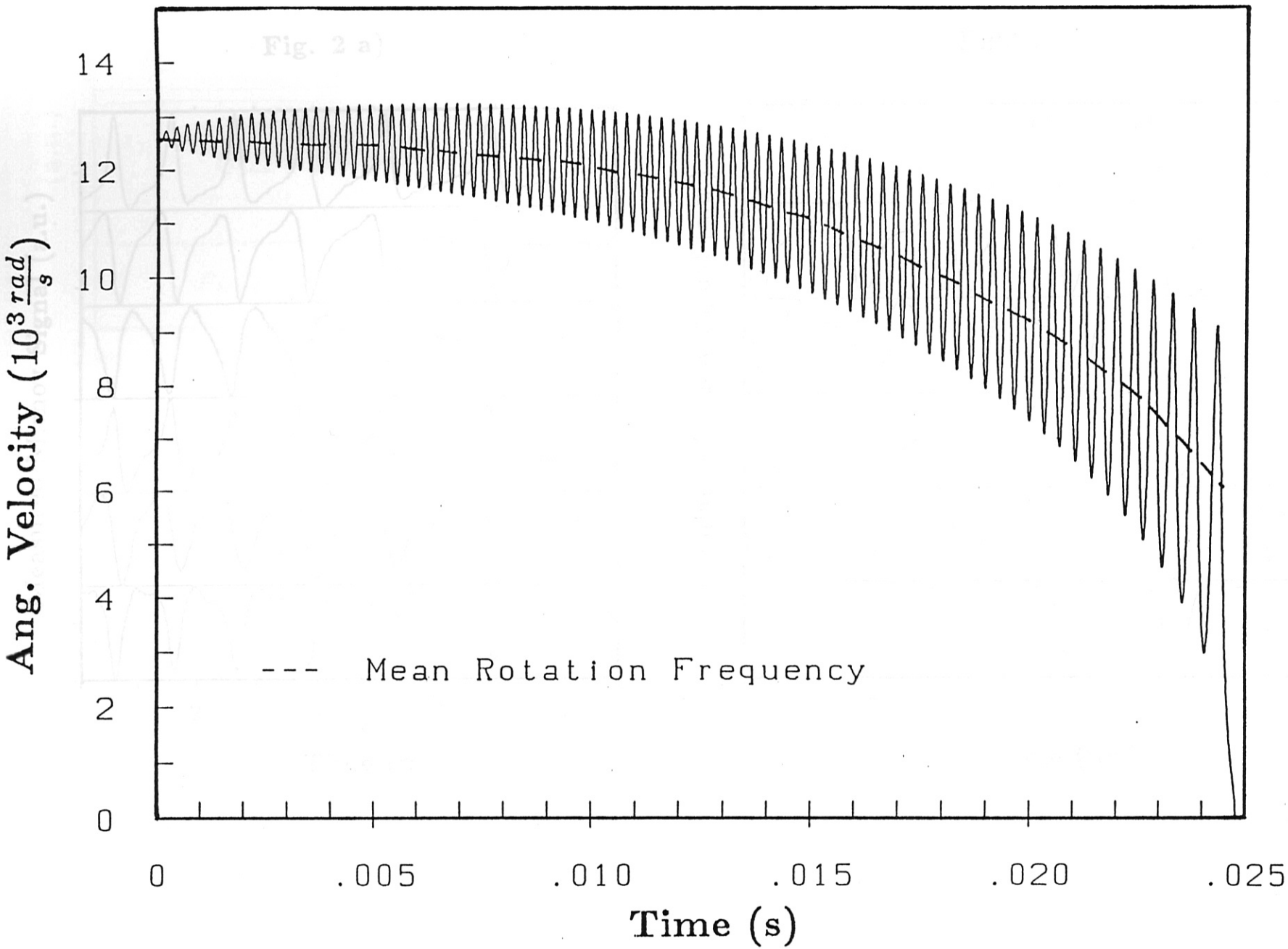
14
12
10
8
6
4
2
0
Ang. Velocity ($10^3 \frac{rad}{s}$)
--- Mean Rotation Frequency
0
.005
.010
.015
.020
.025
Time (s)

Fig. 2 a)

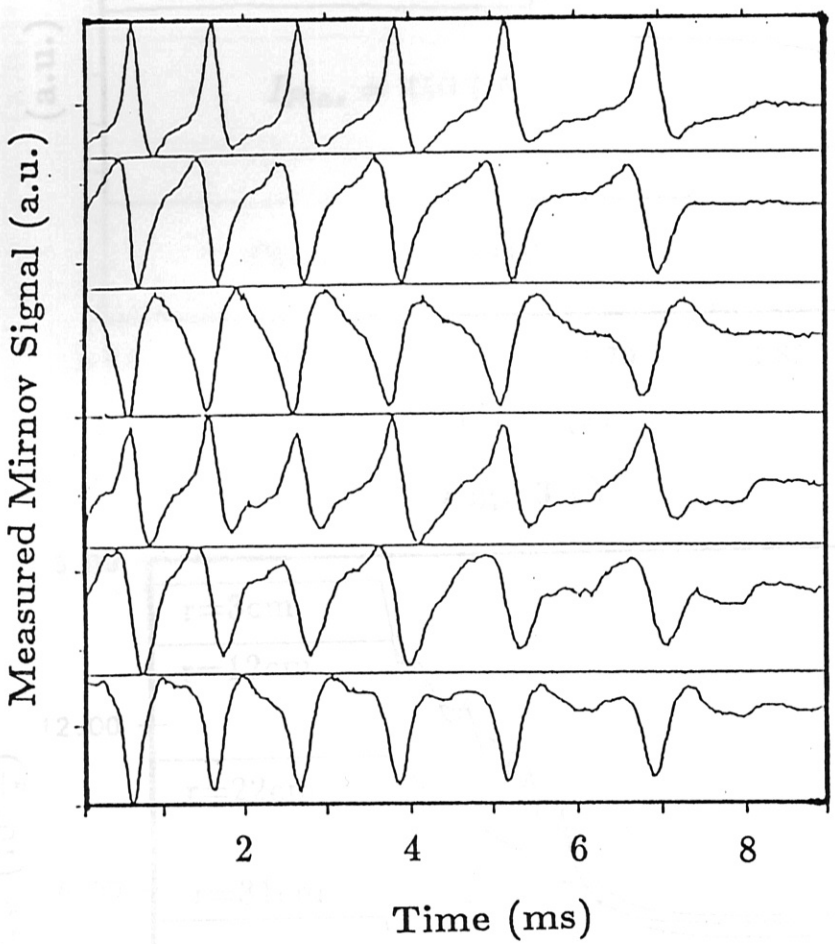
Measured Mirnov Signal (a.u.)
2
4
6
8
Time (ms)

Fig. 2 b)

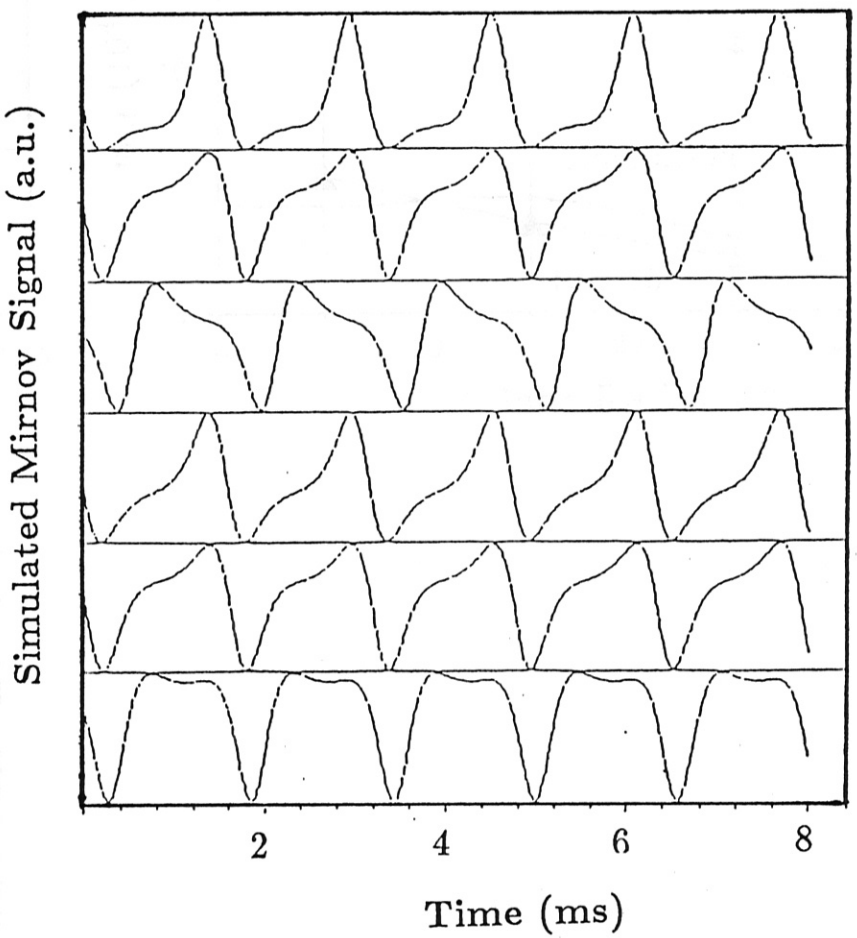
Simulated Mirnov Signal (a.u.)
2
4
6
8
Time (ms)

Fig. 3 a)

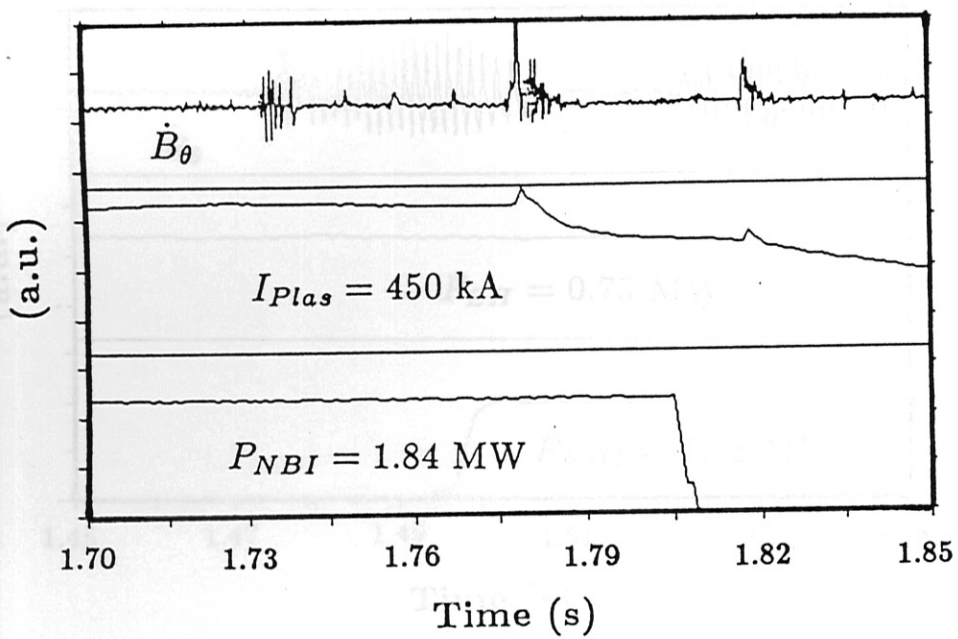

Fig. 3 b)

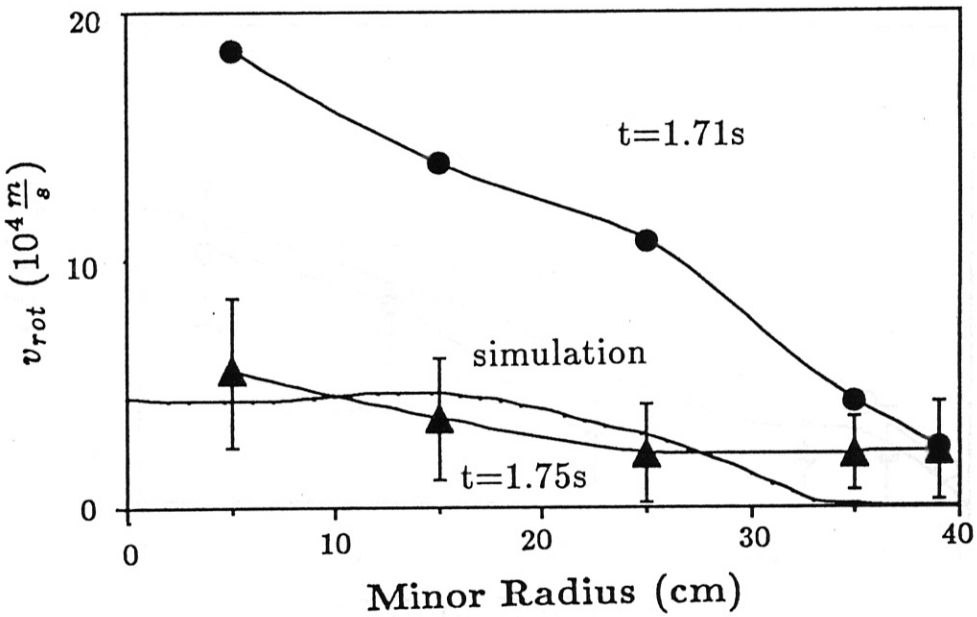

Fig. 3 c)

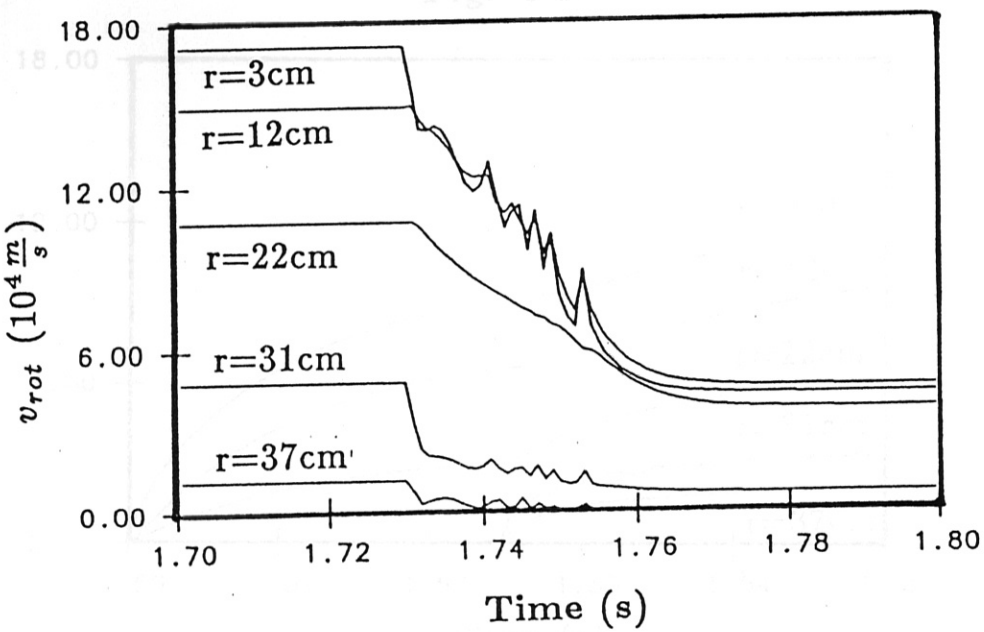

Fig. 4 a)

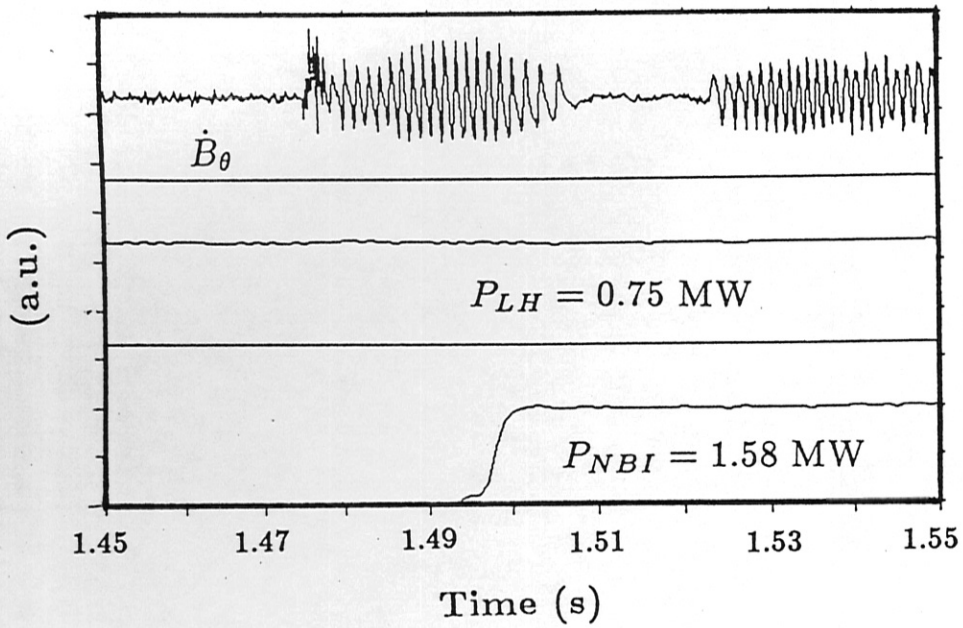

Fig. 4 b)

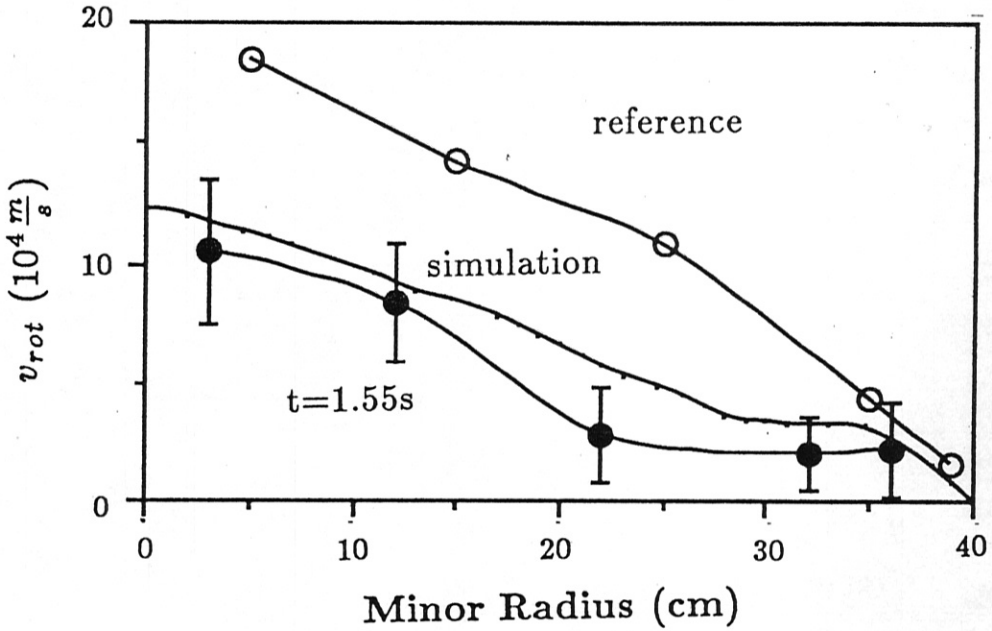

Fig. 4 c)